RESEARCH ARTICLE

Optimization scheme of wind energy prediction based on artificial intelligence

Yagang Zhang [1,2,3] · **Ruixuan Li** [1] · **Jinghui Zhang** [1]

Abstract

Wind energy, as one of the renewable energies with the most potential for development, has been widely concerned by many countries. However, due to the great volatility and uncertainty of natural wind, wind power also fluctuates, seriously affecting the reliability of wind power system and bringing challenges to large-scale grid connection of wind power. Wind speed prediction is very important to ensure the safety and stability of wind power generation system. In this paper, a new wind speed prediction scheme is proposed. First, improved hybrid mode decomposition is used to decompose the wind speed data into the trend part and the fluctuation part, and the noise is decomposed twice. Then wavelet analysis is used to decompose the trend part and the fluctuation part for the third time. The decomposed data are classified. The long- and short-term memory neural network optimized by the improved particle swarm optimization algorithm is used to train the nonlinear sequence and noise sequence, and the autoregressive moving average model is used to train the linear sequence. Finally, the final prediction results were reconstructed. This paper uses this system to predict the wind speed data of China's Changma wind farm and Spain's Sotavento wind farm. By experimenting with the real data from two different wind farms and comparing with other predictive models, we found that (1) by improving the mode number selection in the variational mode decomposition, the characteristics of wind speed data can be better extracted. (2) According to the different characteristics of component data, the combination method is selected to predict modal components, which makes full use of the advantages of different algorithms and has good prediction effect. (3) The optimization algorithm is used to optimize the neural network, which solves the problem of parameter setting when establishing the prediction model. (4) The combination forecasting model proposed in this paper has clear structure and accurate prediction results. The research work in this paper will help to promote the development of wind energy prediction field, help wind farms formulate wind power regulation strategies, and further promote the construction of green energy structure.

Keywords Short-term wind speed prediction · Variational mode decomposition · Improved particle swarm optimization · Long- and short-term memory neural network · Autoregressive moving average model · Noise decomposition

Introduction

In recent years, with the rapid development of national economy and society, the demand for electric energy is gradually expanding, and the traditional fossil energy has caused serious pollution, such as global warming, heat pollution, air pollution, and ecological damage. Countries all over the world have reached a consensus on green development and put forward green development plans, hoping to accelerate the transformation of energy structure and establish a cleaner and more flexible clean energy system. China, the USA, Japan, and other countries have put forward the goal of carbon neutrality in the middle of this century. The transition to a low carbon society is dependent on renewable energy-based electrification (Nazir

et al. 2020a). Wind energy is an important substitute for traditional fossil energy (Nazir et al. 2020b). According to the latest data, in 2019, the global installed 176 GW of new renewable energy (just under 2018 new 179 GW), accounting for 72% of the world's new generating capacity, renewable energy share in the global electricity generation rose to 34.7% from 33.3% at the end of 2018 (International Renewable Energy Agency's 2020).

Wind energy is inexhaustible, with low development cost and clean (Chaurasiya et al. 2019). Wind power in China has been given full attention by the government and developed rapidly. According to the latest data of the national energy administration, in the first three quarters of 2020, the new installed capacity of wind power in China will be 13.92 million kilowatts, including 12.34 million kilowatts on land and 1.58 million kilowatts on the sea. By the end of the third quarter of 2020, the total installed capacity of wind power in China will be 223 million kilowatts, including 216 million kilowatts of onshore wind power and 7.5 million kilowatts of offshore wind power. At present, China has become the largest wind power market in the world (National Energy Administration 2020).

With the rapid development of the wind power industry, the height of wind turbines has gradually increased. Although the height limitation of mast technology has been solved, its installation cost and maintenance have become expensive and cumbersome. Thus, SODAR and LIDAR technologies are used to replace wind turbines in complex regions to measure wind speed, which improves the credibility of wind speed data and reduces power generation costs. At the same time, the nonlinear relationship between wind power and wind speed determines the accuracy of wind speed modeling and has a direct impact on wind power generation (Prem Kumar Chaurasiya et al. 2017; Chaurasiya et al. 2018a). However, wind speed has high random fluctuation and intermittency, which leads to high random fluctuation of wind power. Large-scale wind power grid connection will bring challenges to power system safety and power quality. And accurate wind speed prediction can help control wind power output, power plant wind power safety scheduling, and other issues; therefore, wind speed prediction has very important theoretical significance and practical value.

Currently, wind speed prediction methods can be generally divided into physical model method (Higashiyama et al. 2018; Harty et al. 2019), statistical model method (Erdem and Shi 2011; Nourani Esfetang and Kazemzadeh 2018; Chaurasiya et al. 2018b), and artificial intelligence (Sharifian et al. 2018; Chitsaz et al. 2015). The physical model method makes wind speed prediction by calculating the terrain, air pressure, climate, and other information around the wind farm, and the data obtained is generally used as input for other statistical models. The statistical model method uses the historical wind speed data to establish the statistical model and obtain the wind speed time series; artificial intelligence method uses ANN, SVM, and other methods to predict wind speed

according to the characteristics of historical wind speed data. Nowadays, BP (Zhao et al. 2014; Wang et al. 2019; Li et al. 2019a; Glowacz and Glowacz 2018), LSTM (Gu et al. 2020; Shahid et al. 2020), RBF (Tang et al. 2020; Cao et al. 2019; Zhang et al. 2015), Elman (Yu et al. 2017; Li et al. 2019b), and so on are widely used and have excellent effect. Zendehboudi et al. (2018) used SVM as the basic model. Wang et al. (2016) used BP neural network as the basic model. Wu et al. (2015) used RBF neural network as the basic model for wind speed prediction. The prediction results were generally better than statistical model method (Yuan et al. 2015; Zafirakis et al. 2019). To improve the algorithm of single neural network is a widely used method to improve the accuracy of prediction (Zhang et al. 2019a; Tian et al 2019). Therefore, in this paper, IPSO is used to improve the LSTM neural network prediction model. All kinds of wind speed prediction methods have their own advantages and disadvantages. Compared with the single prediction model, the combined forecasting model based on artificial intelligence algorithm will be more used in the research of wind speed prediction. Peng et al. (2020) proposes a negative correlation learning-based regularized extreme learning machine ensemble model (NCL-RELM) integrated with optimal variational mode decomposition (OVMD) and sample entropy (SampEn) for multi-step ahead wind speed forecasting. Zhang et al. (2020a) combined artificial intelligence methods with statistical knowledge and proposed an optimized radial basis function model and interval prediction model of the Fourier distribution of wind speed based on FCBF. Zhang and Pan (2020) proposed an RBF-ARMA model based on wind speed characteristics by combining statistical model method and artificial intelligence method. An autoregressive integral moving average model based on repeated wavelet transform is used to improve the accuracy of ARIMA model for short-term wind speed prediction (Bri-Mathias Hodge et al. 2011). A combined forecasting model is established, which is composed of three main modeling steps: quadratic decomposition, integration method, and error correction (Liu et al. 2018a). A new wind speed multi-step prediction framework based on WPD, CEEMDAN, and ANN is proposed (Liu et al. 2018b). It is proved that the performance of the combined model is better than that of the corresponding neural network model.

Wind speed is random and non-stationary. From the perspective of wind speed characteristics, the commonly used signal processing methods include principal component analysis (Skittides and Früh 2014), wavelet transform (Dang et al. 2013; Zhang et al. 2020b), EMD (Wang et al. 2016; Dragomiretskiy and Zosso 2014), and its improved EEMD, WPD, and VMD (Zhang et al. 2019b). In the process of obtaining the decomposed components, VMD determines the frequency center and bandwidth of each component by iteratively searching for the optimal solution of the variational model, so as to realize the frequency domain segmentation of the signal and the effective separation of

each component adaptively. Because VMD overcomes the endpoint effect and modal aliasing of EMD and has good decomposition effect, it has been applied to wind speed sequence decomposition. Zhang et al. (2020c) used VMD to decompose the original wind speed and compared with EMD method to verify that VMD has a better decomposition effect. In view of the inconvenient choice of mode number K in VMD, Chen (2020) selects the appropriate decomposition times K by judging the value of sample entropy. From the perspective of energy, Chen (2020) proposed an energy difference component selection method to calculate the number of comparative mode decomposition. Combined with the singular value decomposition (SVD) difference spectrum processing error, a hybrid HMD data processing method is constructed. This method improves the quality of decomposition and overcomes the defect of random mode number selection. Experiments show that HMD method is better than VMD method.

Therefore, based on the improved VMD method and IPSO-LSTM neural network, a new wind speed prediction scheme is designed. The specific process is as follows:

Firstly, data preprocessing is used to extract data features. The SVD differential spectrum is used to denoise, MIV and PCA are used for multi factor analysis, and the energy difference mode number selection method is used to optimize the VMD mode number, and VMD decomposition is carried out. After the decomposition, WT is used to decompose the modal components again.

Then the decomposed time series are classified, and the nonlinear time series are trained and predicted by LSTM neural network, and the linear time series are trained and predicted by ARMA model. In this paper, fitting interpolation is used to predict the noise sequence.

Finally, each predicted value is reconstructed to obtain the final prediction result.

The rest of this paper is arranged as follows: Section 2 introduces the improved VMD method used in this paper; Section 3 introduces IPSO-LSTM model and ARMA model; Section 4 introduces the forecast flow of the wind speed forecast scheme described in this paper; Section 5 uses this prediction scheme to predict the real wind farm data, compares the results of China's Changma wind farm and Spain's Sotavento wind farm, and makes comparisons with other schemes; Section 6 draws the conclusions.

The improved VMD method

Singular value difference spectrum

Let the time series $V(t) = [v(1), \cdots, v(t)]$ with noise constitute Hankel matrix of $m \times n$ order, and make the matrix as square as possible, so as to achieve better noise reduction effect.

$$H = \begin{pmatrix} v(1) & v(2) & \cdots & v(n) \\ v(2) & v(3) & \cdots & v(n+1) \\ \vdots & \vdots & \ddots & \vdots \\ v(m) & v(m+1) & \cdots & x(t) \end{pmatrix} \quad (1)$$

By singular value decomposition of V, we can get the following result:

$$H = U_{m \times n} \Sigma_{n \times n} V_{n \times n}^T \quad (2)$$

where $U_{m \times n}$, $V_{n \times n}$ is an orthogonal matrix, Σ is a nonnegative diagonal matrix, and the non-zero value on the diagonal of Σ is the singular value of H.

There are k singular values, which are sorted as follows

$$\sigma = (\sigma_1, \cdots, \sigma_k) \quad (3)$$

where σ_i is the i-th singular value after sorting (i is from 1 to k).

The singular value mutation of noisy sequences can be well expressed by using differential spectrum:

$$d_i = \sigma_i - \sigma_{i-1}, i = 1, 2, \cdots, r-1 \quad (4)$$

The order P of reconstruction can be determined by the point with the largest singular value mutation, and the denoising sequence and noise sequence can be obtained finally.

$$V(t) = x_1(t) + r_1(t) \quad (5)$$

where $x_1(t)$ is the denoising sequence and $r_1(t)$ is the noise sequence.

Variational mode decomposition

The VMD method was proposed by Dragomiretskiy and others. It was originally used to analyze the early failure of rolling bearings. Because this method overcomes a series of shortcomings of EMD mode aliasing and endpoint effect and has good decomposition effect and good noise robustness, it is introduced into wind speed prediction to decompose wind speed time series. According to the center frequency and bandwidth of each decomposition component, the frequency domain decomposition of the signal and the effective separation of each component are realized (Glowacz 2018; Glowacz 2019).

The VMD first constructs the variational problem. Let the original time series be decomposed into k components to ensure that the decomposed sequence is a modal component with a finite bandwidth and a central frequency. At the same time, the sum of estimated bandwidth of each mode is the minimum. The constraint condition is that the sum of all

modes is equal to the original signal:

$$\left\{ \min_{\{u_k\}\{w_k\}} \left\{ \sum_k \left\| \partial_t \left[\left(\delta(t) + \frac{j}{\pi t} \right) * u_k(t) \right] e^{-j\omega_k t} \right\|_2^2 \right\} s.t. \sum_k u_k(t) = x(t) \right.$$

(6)

where K is the number of modes to be decomposed, $\{u_k\}$ $\{w_k\}$ is the $k-th$ mode component and center frequency after decomposition, ∂_t is the pair function $\varphi_k(t)$ find the partial derivative of t, $\delta(t)$ is Dirichlet function, $*$ is convolution, and $x(t)$ is the original input signal.

Then, by introducing the Lagrange multiplication operator λ, the constrained variational problem is transformed into an unconstrained variational problem.

Then, Eq. (6) is solved, and the Lagrange multiplication operator λ is introduced to transform the constrained variational problem into a non-constrained variational problem. The expression of augmented Lagrange is:

$$L(\{u_k\}, \{\omega_k\}, \lambda(t))$$

$$= \alpha \sum_k \left\| \partial_t \left[\left(\delta(t) + \frac{j}{\pi t} \right) * u_k(t) \right] e^{-jw_k t} \right\|_2^2$$

$$+ \left\| x(t) - \sum_k u_k(t) \right\|_2^2 + \left[\lambda(t), x(t) - \sum_k u_k(t) \right]$$

(7)

In the formula, α is the quadratic penalty factor to reduce the interference of Gaussian noise. Alternate wind direction multiplier iterative algorithm combined with Parseval/Plancherel and Fourier equidistance transform is used to optimize to obtain each modal component and center frequency and to search the saddle points of the augmented Lagrange function.

The expressions of $\{u_k\}$, $\{\omega_k\}$, $\lambda(t)$ after alternating optimization iteration are shown in Formula (8), (9), and (10):

$$\widehat{u}_k^{n+1}(\omega) = \frac{\widehat{x}(\omega) - \sum_{i<k} \widehat{u}_i^n(\omega) + \frac{\widehat{\lambda}(\omega)}{2}}{1 + 2\alpha(\omega - \omega_k)^2}$$

(8)

$$\omega_k^{n+1} = \frac{\int_0^\infty \omega \left| \widehat{u}_k^{n+1}(\omega) \right|^2 d\omega}{\int_0^\infty \left| \widehat{u}_k^{n+1}(\omega) \right|^2 d\omega}$$

(9)

$$\widehat{\lambda}^{n+1}(\omega) = \widehat{\lambda}^n(\omega) + \gamma \left(\widehat{f}(\omega) - \sum_k \widehat{u}_k^{n+1}(\omega) \right)$$

(10)

If the convergence satisfies the condition (11), the iteration is finished:

$$\sum_k \left\| \widehat{u}_k^{n+1} - \widehat{u}_k^n \right\|_2^2 / \left\| \widehat{u}_k^n \right\|_2^2 < \varepsilon$$

(11)

where ε is the set precision.

Modal number selection method

In order to make up for the deficiency in subjective selection of influencing parameters, Bing (2020) proposed a modal number selection strategy to overcome the defects caused by random selection of modal numbers, and strict experiments proved that the use of HMD was superior to VMD method.

From the optimal theoretical result of VMD decomposition, the sum of the energies of each component is equal to the original signal. When k value is too large, the generation of the fictitious component will cause the energy sum of the components to be too high. Based on this principle, according to the calculation (Formula (12)) of wind speed signal energy and energy difference, when the value of $\theta_{k, k-1}$ is small, the signal will be underdecomposed. With the increase of the value of $\theta_{k, k-1}$, VMD is overdecomposed obviously. Therefore, with the increase of parameters k, there will be decomposition phenomenon, and the corresponding value $\theta_{k, k-1}$ will increase significantly. In this case, it can be regarded $k-1$ as the optimal mode number of VMD decomposition.

$$\begin{cases} E_k^l = \sqrt{\frac{\sum_{i=1}^n x_l^2(i)}{n}}, l = 1, 2, \cdots k \\ E_k = \sum_{l=1}^k E_k^l \\ \theta_{k,k-1} = \frac{|E_k - E_{k-1}|}{E_{k-1}} \end{cases}$$

(12)

where E_k is the energy sum of all components when the mode number is k, E_{k-1} is the sum of component energies after the last decomposition, $\theta_{k, k-1}$ represents the energy difference, $x_l(i)$ is the $l-th$ component sequence under the current mode number, and n is the number of sampling points.

IPSO-LSTM model and ARMA model

### Improved particle swarm optimization

The LSTM model is based on the deep neural network, which is very complex to set and optimize the hyperparameters. In this paper, the particle swarm optimization (PSO) algorithm is used to optimize the super parameters in the model. The PSO algorithm has the advantages of simple principle, small consumption of computing resources, good convergence, and high computational efficiency.

The speed and position update formula of PSO algorithm is as follows:

$$\begin{cases} V_{id}^{t+1} = \omega V_{id}^t + c_1 r_1 (P_{id} - X_{id}^t) + c_2 r_2 (Q_{id} - X_{id}^t) \\ X_{id}^{t+1} = V_{id}^{t+1} + X_{id}^t \end{cases}$$

(13)

where ω is the inertia weight, c_1, c_2 is the learning factor, r_1, r_2 is an independent random number distributed between [0,1], V_{id}^t represents the velocity component of the ith particle in d

Fig. 1 Cell update process of LSTM
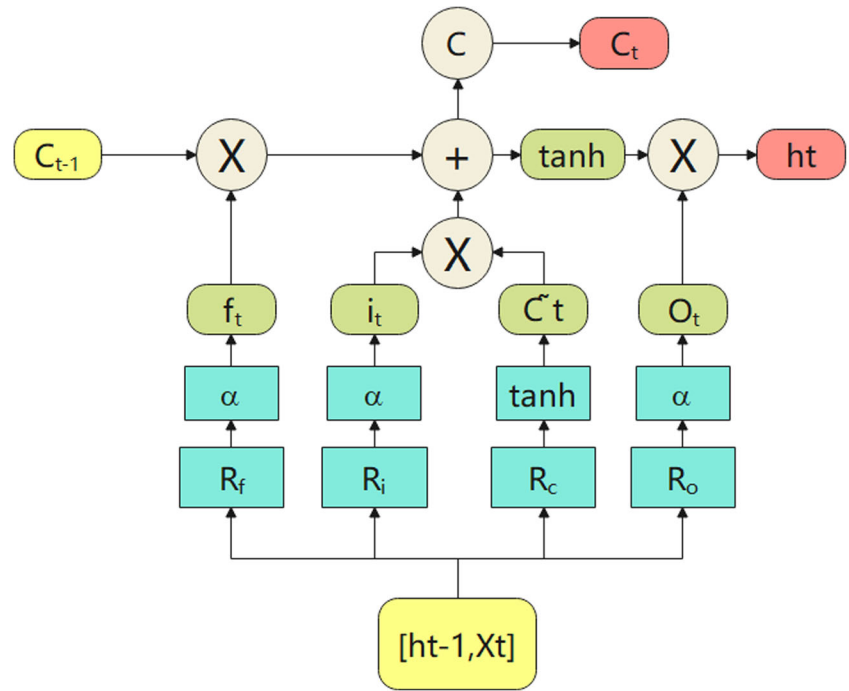
dimension in the t iteration, X_{id}^t represents the position component of the ith particle in d dimension in the t iteration, P_{id} represents the individual optimal value of the ith particle in $d$dimension in the t iteration, and Q_{id} represents the population global optimal value of the ith particle in d dimension in the t iteration.

But PSO algorithm has the phenomenon of local optimum, premature convergence, or stagnation, so it needs to be improved. This paper proposes that the learning factors change linearly with evolution, such as Formula (14). In this way, the particles can move in the whole search space in the early stage of optimization and move around the optimal solution in the late stage of optimization, so as to improve the convergence rate of the optimal solution. The inertia weight decreases nonlinearly with evolution, as shown in Formula (15). In this way, the search speed is gradually reduced, and the algorithm convergence is convenient.

$$\begin{cases} c_1 = a_1 + a_2 l / L_{max} \\ c_2 = a_3 - a_4 l / L_{max} \end{cases} \quad (14)$$

$$\omega(l) = \omega_{max} - (\omega_{max} - \omega_{min}) * arcsin \frac{l}{L_{max}} * \frac{2}{\pi} \quad (15)$$

where l is the number of iterations, L_{max} is the maximum number of iterations allowed, and a_1, a_2, a_3, a_4 are constants.

Long- and short-term memory neural network

The RNN has memory, parameter sharing, and Turing completeness, which has certain advantages in learning the nonlinear characteristics of sequences. With the development of

deep learning technology, the concept of time series has also been applied in the structural design of RNN. Therefore, RNN has good time series analysis capability. As an improved RNN, LSTM inherits RNN's ability to analyze time series data while enhancing long-term memory. LSTM neural network model has been applied in the field of wind speed prediction because it can keep memory for a long time effectively.

All RNNs have a chain structure of repetitive neural network modules, which is a simple structure in standard RNN. But there are three gates in the memory unit of LSTM neural network, which are input gate, forget gate, and output gate. The calculation process of LSTM update unit is as follows:

Input gate

The information passed first is input at t, and then the value of input layer of memory unit is updated to i_t:

$$i_t = \alpha_i (R_i \cdot [h_{t-1}, x_t] + b_i) \quad (16)$$

The candidate value of hidden layer state is updated as $\widetilde{C}_t$:
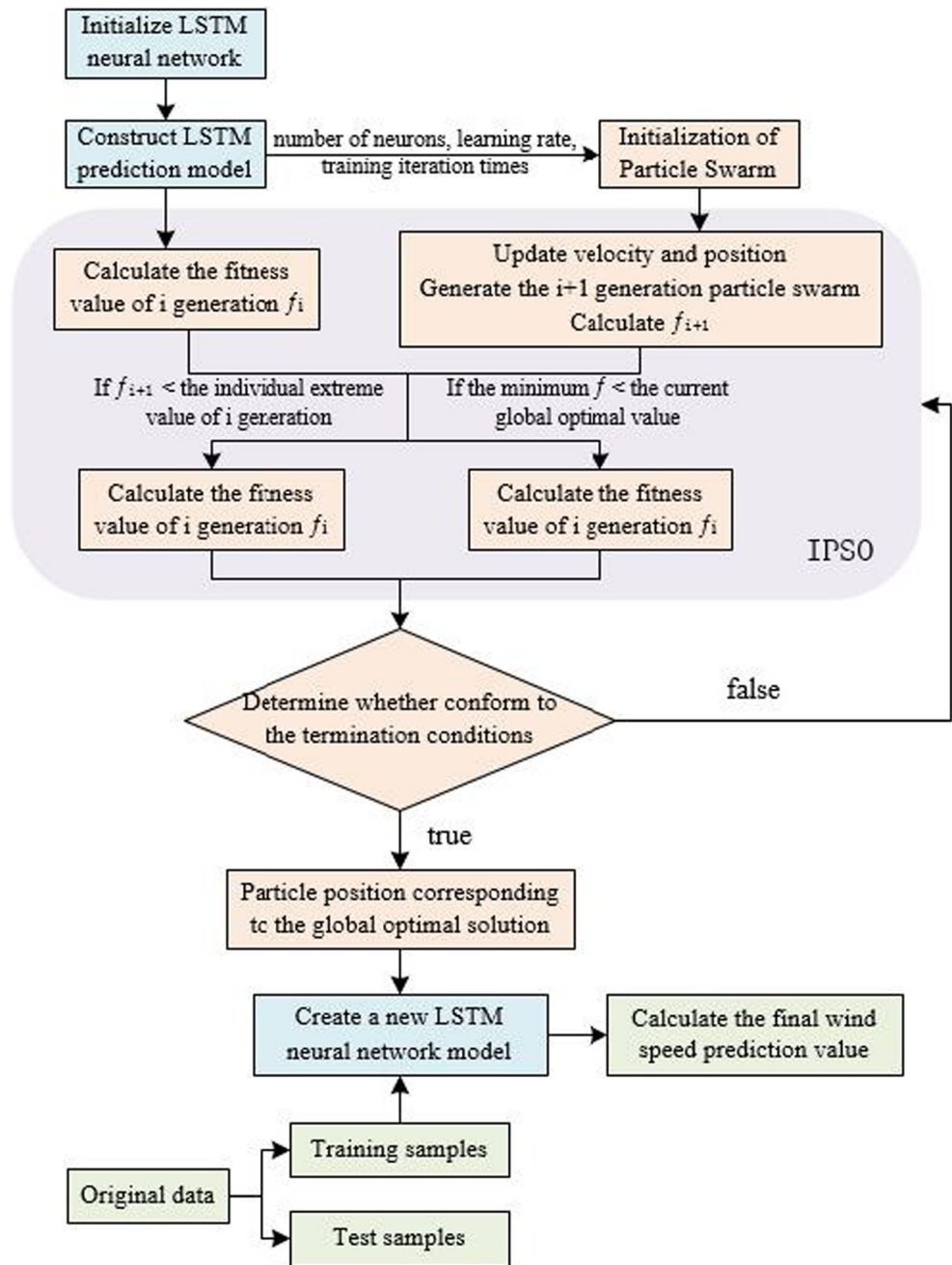
$$\widetilde{C}_t = tanh(R_C \cdot [h_{t-1}, x_t] + b_C) \quad (17)$$

Forgetting gate

The value of forgetting layer in memory unit is f_t:

$$f_t = \alpha_f (R_f \cdot [h_{t-1}, x_t] + + b_f) \quad (18)$$

Fig. 2 IPSO-LSTM flow chart

At this point, the status update value of the hidden layer is C_t:

$$C_t = f_t * C_{t-1} + i_t * \widetilde{C}_t \tag{19}$$

Output gate

The value of the output layer and the output value of the final memory unit are updated to o_t, h_t:

$$o_t = \alpha_o(R_o \cdot [h_{t-1}, x_t] + b_o) \tag{20}$$

$$h_t = o_t * tanh(C_t) \tag{21}$$

where x_t is the input vector, h_t is the output vector, α represents the gate activation function, $*$ is the element multiplication between two vectors, R represents the corresponding weight matrix, and b is the relevant partial vector.

The cell update process diagram is shown in Fig. 1.

Process of IPSO optimizing LSTM

Step 1: Initialize LSTM neural network. The input and output data are selected and normalized to create LSTM

neural network. The number of neurons in each layer, learning rate, and training iteration times are determined.

Step 2: Initialization of particle swarm. The particle swarm size is determined, and the particle velocity v_0, position x_0, inertia weight ω, learning factors c_1, c_2, maximum iteration number L_{max}, minimum inertia weight ω_{min}, maximum inertia weight ω_{max}, minimum velocity v_{min}, and maximum velocity v_{max} are initialized.

Step 3: Construct LSTM prediction model and determine the optimization range of parameters. The number of neurons in each layer, learning rate, and training iteration times are taken as parameter variables to determine the optimization range of parameters. The original data is divided into training samples and test samples.

Step 4: Define the fitness value f_i of LSTM model as:

$$f_i = \frac{1}{2}\left(\frac{1}{P}\sum_{p=1}^{p}\frac{y_p - \widehat{y}_p}{y_p} + \frac{1}{Q}\sum_{p=1}^{p}\frac{y_q - \widehat{y}_q}{y_q}\right) \tag{22}$$

where P, Q are the number of training samples and test samples, y_p, $\widehat{y}_p$ are the true value of the training sample and the test paper, and y_q, $\widehat{y}_q$ are the true value and predicted value of the validation sample.

Step 5: Update and calculate the velocity and position of each particle, generate the next generation of particle swarm, and calculate the individual and global extremum of the next generation particle swarm. The fitness value of particles is calculated. If the current fitness value of particles is less than the individual extreme value of the previous generation, the individual extreme value and individual optimal position are updated; if the minimum fitness value of all particles is less than the current global optimal value, the global optimal value and global optimal position are updated.

Step 6: Judge whether the termination conditions are met. If the training reaches the maximum number of times or the training error meets the accuracy requirements, the iteration is terminated, and the particle

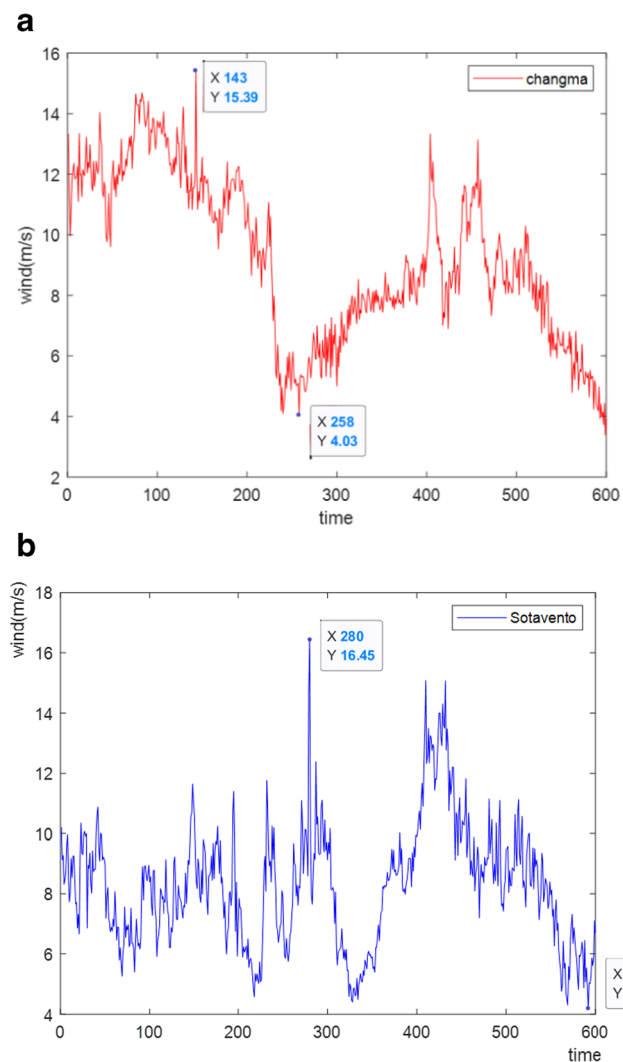**Fig. 3** Combination forecasting scheme

a

b
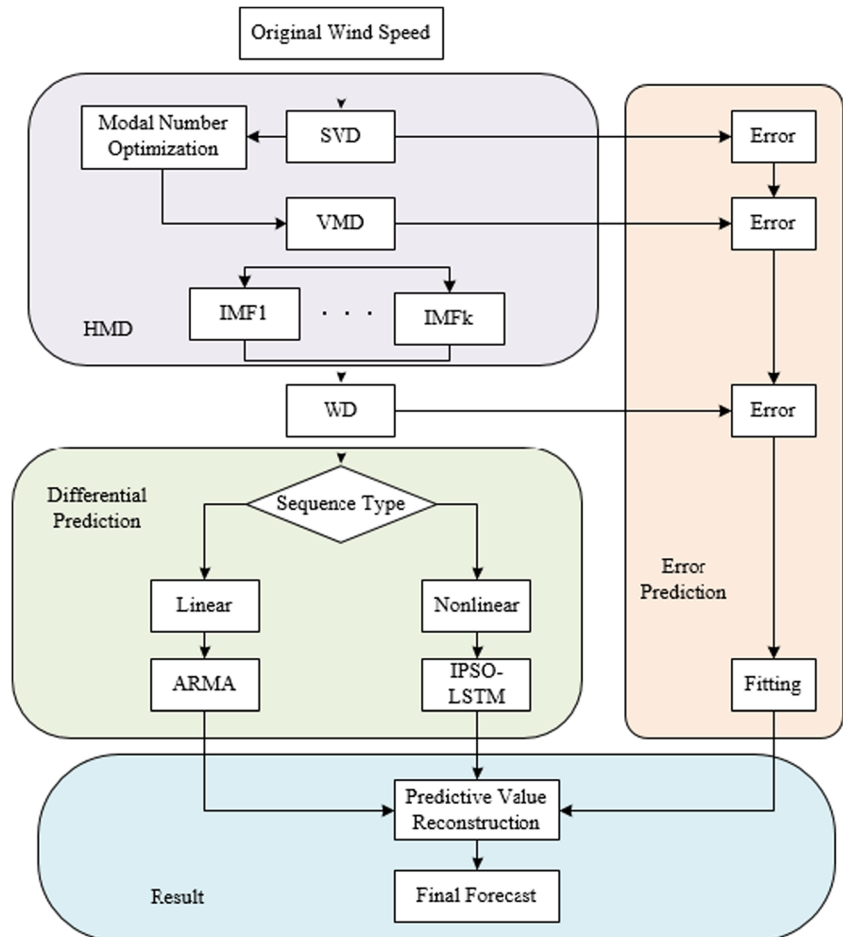
Fig. 4 (**a**–**b**) Wind speed data of different wind farms. (**a**) Wind speed of Changma Wind Farm in China. (**b**) Wind speed of Sotavento wind Farm in Spain
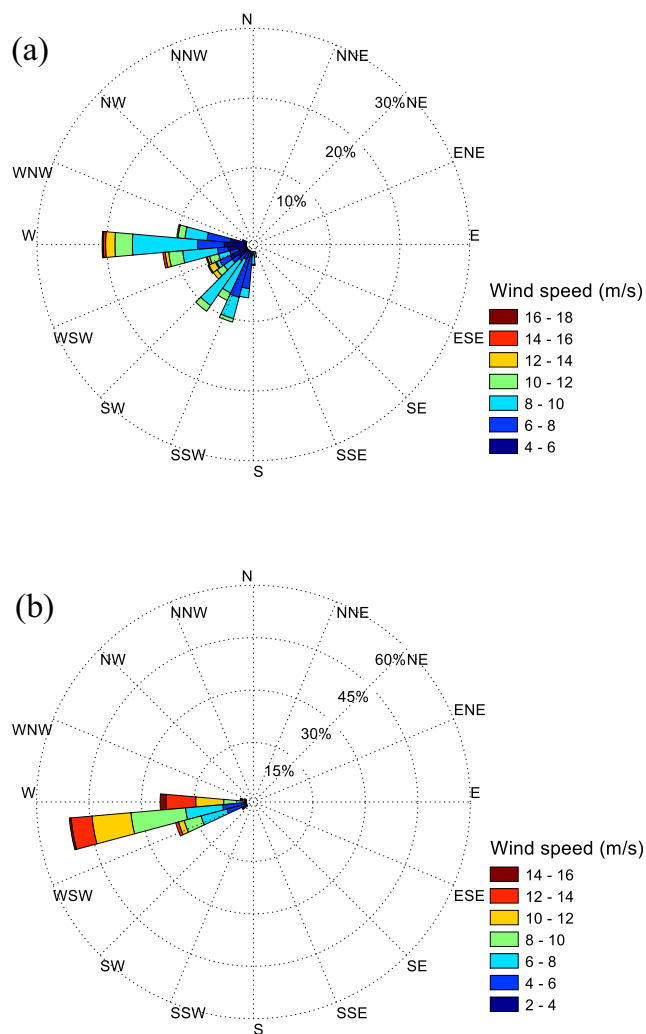
(a)

(b)

Fig. 5 (**a**–**b**) Wind rose chart of different wind farms. (**a**) Wind rose chart of Sotavento wind Farm in Spain. (**b**) Wind rose chart of Changma wind farm in China

$\{e_t\}$ is white noise, $\phi_1\cdots\phi_p,\theta_1\cdots\theta_q$ is regression parameter, and p and q are autoregressive coefficient and moving average order. If $\phi_1\cdots\phi_p,\theta_1\cdots\theta_q$ is not all 0, then the sequence $\{Y_t\}$ is called autoregressive moving average mixing process, which is called $ARMA\,(p,q)$.

Combination forecasting scheme

In this paper, 600 data from China's Changma wind farm and Spain's Sotavento wind farm were used, 500 data of which were intercepted as training sets, and the last 100 data were used as test sets. The specific steps are as follows:

Step 1. The SVD differential spectrum is used to decompose the original wind speed data for the first time, and the original wind speed data is changed into two parts:

position corresponding to the final global optimal solution is output. Otherwise, go to step 5.

Step 7: Using the optimized parameters of LSTM neural network model, a new LSTM neural network model is created. Input the training set and calculate the final wind speed prediction value.

The flow chart of IPSO-LSTM is shown in Fig. 2:

ARMA model

ARMA model is a basic model for time series analysis.

Let the time series $\{Y_t\}$ is a linear difference equation,

$$Y_t - \phi_1 Y_{t-1} - \phi_2 Y_{t-2} - \cdots - \phi_p Y_{t-p}$$
$$= e_t - \theta_1 e_{t-1} - \theta_2 e_{t-2} - \cdots \theta_q e_{t-q} \qquad (23)$$
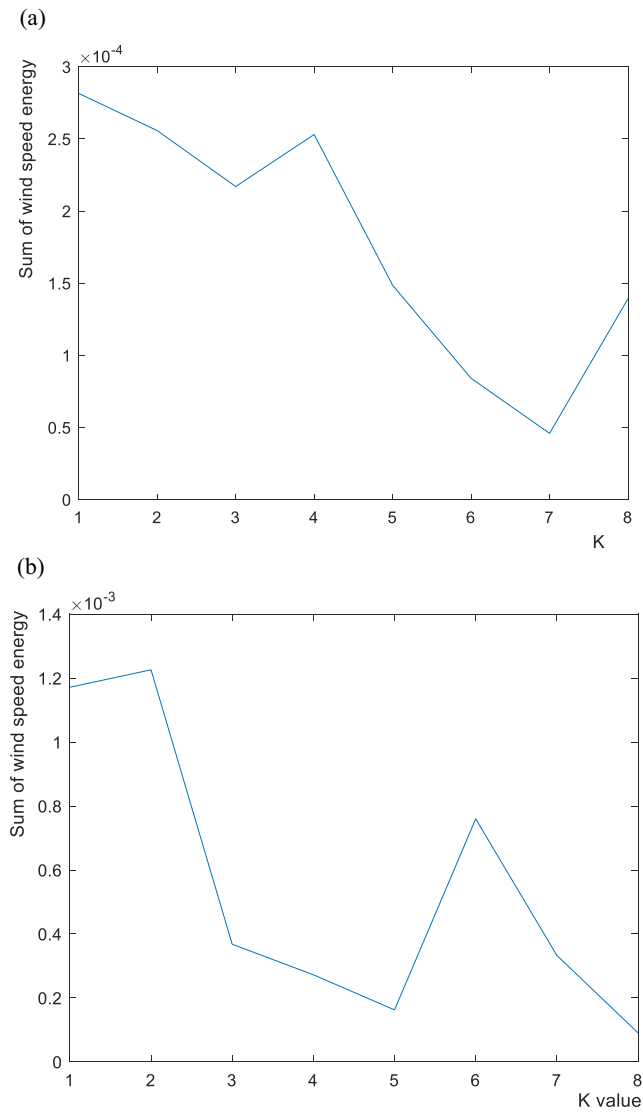
(a)

(b)

Fig. 6 (**a–b**) Sum of wind speed energy decomposed by VMD of different wind farms. (**a**) Sum of wind speed energy decomposed by VMD in Changma wind farm. (**b**) Sum of wind speed energy decomposed by VMD in Sotavento wind farm

noise reduction sequence $x_1(t)$ and noise sequence $r_1(t)$.

Step 2. MIV screening and PCA were used for multivariate analysis. Use the energy difference modal number optimization method to calculate the energy difference between different modal numbers and select k value.

Table 1 Energy difference between different modes ($\times 10^{-4}$)

Modal number	3.4	4.5	5.6	6.7	7.8
E/Sotavento	−0.9	−1.1	6.0	−4.3	−5.7
E/Changma	0.4	−1.1	−0.6	−0.4	0.9

Step 3. The SVD noise reduction sequence is decomposed into k components, namely, $IMF1$, $\cdots$, $IMFk$. At the same time, the noise $r_2(t)$ is proposed.

$$r_2(t) = x_1(t) - IMF1 - \cdots - IMFk \qquad (24)$$

Step 4. Wavelet decomposition is used to decompose each component again to get the denoising sequence $x_3(t)$ and noise sequence $r_3(t)$.

Step 5. Analysis of denoising sequence $x_3(t)$. Using IPSO-LSTM neural network to train nonlinear sequence and ARMA model to train linear series, the prediction result of denoising sequence is y_1, $\cdots$, y_k.

Step 6. The noise sequence is fitted with probability distribution. The results show that the data obey normal distribution. The result of noise analysis y_r can be made up of random numbers from the normal distribution of error sequence.

Step 7. Reconstruct the predicted value to get the final prediction result.

$$y = y_1 + y_2 + \cdots + y_k + y_r \qquad (25)$$

The flow chart is shown in Fig. 3:

Experiment

Data analysis

In this paper, wind speed data of Changma wind farm in China and Sotavento wind farm in Spain were used for analysis. The data of Sotavento wind farm include wind speed, wind direction, air temperature, air pressure, specific volume, specific humidity, and surface roughness; the environmental factors of China Changma wind farm include wind direction, air temperature, motor speed, and pitch angle. The hub height of Sotavento wind farm and Changma wind farm is 45m and 65m, respectively. Six hundred data were selected for training with a sampling interval of 10min. The first 500 data were taken as training samples, and the last 100 data were taken as test sets.

The original wind speed diagram is shown in Fig. 4. Figure 4a shows the wind speed data of the Changma wind farm in China, and Fig. 4b shows the wind speed data of the Sotavento wind farm in Spain. It can be seen from the figure that the wind speed of Changma Wind Farm in China has a strong random volatility and no obvious periodic characteristics within the range of 4m/s, 16m/s, while the wind speed of Sotavento in Spain has a strong random volatility and no obvious periodic characteristics within the range of 4m/s, 17m/s.

Table 2 MIV value of Sotavento wind farm

Factor	Wind speed	Wind direction	Air temperature	Air pressure	Specific volume	Specific humidity	Surface roughness
MIV	0.4113	−0.2264	−0.1286	0.2492	−0.1093	0.1769	−0.1135

Figure 5 shows the wind rose for two different wind farms. The wind rose diagram shows the wind direction and the wind frequency in this direction, which is convenient for readers to understand the wind data. In this wind data, it can be seen from Fig. 5a that the main wind directions of Sotavento wind farm are west wind and south wind. It can be seen from Fig. 5b that west wind is the main wind direction in Changma wind farm.

Data processing

Firstly, SVD difference spectrum is used for the first error decomposition to extract the periodic features in the original wind speed data and obtain the denoising sequence and noise term.

Then use the formula to calculate the energy of the wind speed sequence after preliminary to remove noise and the results are shown in Fig. 6. It can be seen from Fig. 6a that the energy at $k = 8$ is higher than that at $k = 7$, and the change range is obvious. Therefore, the mode number of the wind speed sequence VMD of Changma wind farm is 7. It can be seen from Fig. 6b that the energy at $k = 6$ increases significantly compared with that at $k = 5$. Therefore, the mode number of VMD of the wind speed series of Sotavento wind farm in Spain is selected as 5.

It can be seen from Table 1 that when the modal number changes from 5 to 6 in Sotavento wind farm, the energy of the denoising sequence after decomposition changes greatly; that is, the energy difference becomes larger. Therefore, the mode number of VMD is 5. Similarly, in Changma wind farm, when the mode number changes from 7 to 8, the energy difference becomes larger. Therefore, the mode number of VMD is 7.

In order to improve the prediction accuracy, we use MIV method to deal with multiple factors. Firstly, the results of MIV among multiple factors are shown in Table 2 and Table 3. We filter out the environmental factors that have little influence on the wind speed prediction results of Sotavento and Changma wind farms, that is, temperature, specific

volume, and surface roughness of Sotavento wind farm and pitch angle of Changma wind farm.

Then, the other factors are analyzed by principal component analysis, and all the principal components whose cumulative variance contribution rate reaches 85% are selected as the fixed inputs of the prediction model. The results are shown in Table 4. Both wind farms choose the first three principal components to participate in the prediction.

After determining the mode number of VMD decomposition, the wind speed series after noise removal is directly decomposed into trend sequence part and fluctuation sequence part, as shown in Fig. 7. Figure 7a shows the VMD decomposition data of Changma wind farm. Figure 7b shows the decomposition data of VMD wind speed of Sotavento wind farm.

Wavelet decomposition is used to decompose the noise of the decomposed IMFs for the last time. The final wind speed sequence which can be used for training is obtained.

Wind Speed prediction

A unit of LSTM neural network contains three gates. This structure can effectively alleviate the gradient disappearance problem and is more suitable for solving nonlinear time-varying problems. Therefore, IPSO-LSTM is used to predict the trend part of the wind speed sequence. The ARMA model is used to train the linear sequence.

Figure 8 shows the variation of fitness values when using IPSO and PSO to optimize the parameters of LSTM neural network using two different wind farm data. It can be seen from Fig. 8a that IPSO converges faster. When using the same parameters, it can be seen from Fig. 8b that PSO has fallen into obvious local convergence. Therefore, the improvement of PSO is necessary and successful.

The wind speed prediction results of Changma wind farm are shown in Fig. 9a, and the wind speed prediction results of Sotavento wind farm are shown in Fig. 9b:

Table 3 MIV value of Changma wind farm

Factor	Wind speed	Wind direction	Air temperature	Motor speed	Pitch angle
MIV	1.4645	0.0188	−0.0426	−0.0544	0.0014

Table 4 Results of PCA

Principal component	Sotavento		Changma	
	Characteristic value	Cumulative variance contribution rate (%)	Characteristic value	Cumulative variance contribution rate (%)
First	1.8101	45.2527	1.6271	61.2153
Second	1.1389	73.7252	0.8211	81.7340
Third	0.7788	93.1942	0.5616	95.7751
Fourth	0.2722	100.0000	0.1690	100.0000

It can be seen from the figure that the IPSO-LSTM-ARMA-E combination prediction is closer to the real value. IPSO-LSTM can predict the trend part of wind speed series better than LSTM. LSTM-ARMA model can predict the peak and trough of wind speed fluctuation more accurately than LSTM neural network. The prediction results of HMD-IPSO-LSTM-ARMA-E model are better than HMD-IPSO-LSTM-E model.

In order to better judge the influence of various variables on the final prediction results and verify the conclusion obtained from direct observation in Fig. 9, it is necessary to conduct accurate error analysis on the prediction results.

In this paper, MAPE, MAE, and MSE are selected to evaluate the model (Hu et al. 2020; Zhang et al. 2021). The calculation formula is Formula (26)

$$\begin{cases} MAPE = \frac{1}{m}\sum_{i=1}^{n}\left|\frac{x_i-\widehat{x}_i}{x_i}\right| \\ MAE = \frac{1}{m}\sum_{i=1}^{n}\left|x_i-\widehat{x}_i\right| \\ MSE = \frac{1}{m}\sum_{i=1}^{n}\left|x_i-\widehat{x}_i\right|^2 \end{cases} \quad (26)$$

where $x_i \; \widehat{x}_i$ is the actual value and predicted value of wind speed at time t and the sample size is m.

The error analysis is shown in Table 5.

It can be seen from the error analysis table that the conclusion obtained from direct observation of Fig. 9 is that HMD-IPSO-LSTM-ARMA-E combination prediction is more accurate and can effectively reduce the error. It can be seen from the table that MAE, MSE, and RMSE are reduced in varying degrees after adding noise prediction. Although the prediction results of HMD-IPSO-LSTM-E model and HMD-IPSO-LSTM model generally have large errors, the noise prediction still effectively reduces the final prediction error, which fully proves the necessity of noise prediction.

To sum up, the prediction results of HMD-IPSO-LSTM-ARMA-E scheme proposed in this paper are closer to the actual values. LSTM-ARMA was used to analyze the differences of different types of time series. IPSO-LSTM optimizes the parameters of LSTM model. Adding error analysis in the

reconstruction of prediction results also reduces the final prediction error. The scheme is feasible.

We take data from Sotavento wind farms in Spain. The first 450 data were taken as training samples, and the last 150 data were taken as test sets. LSTM, RBF, Elman, and BP neural networks are used to predict the data, and the prediction results are as follows (Fig. 10, Table 6):

It can be seen from the error analysis table that LSTM neural network is more suitable for this system. The MAE of LSTM neural network model is 22.5%, 23.5%, and 33.6% less than that of RBF, Elman, and BP neural network model, respectively. The MSE of LSTM neural network model is 38.9%, 41%, and 60.2% less than that of RBF, Elman, and BP neural network model, respectively. The RMSE of LSTM neural network model is 21.9%, 23.4%, and 37.0% less than that of RBF, Elman, and BP neural network model, respectively. Thus, in this experiment, the advantage of LSTM neural network in learning nonlinear sequence has been fully reflected.

Wind speed prediction based on artificial intelligence

When forecasting wind speed, it needs a lot of historical and weather information. Artificial intelligence is the best tool to deal with a lot of data. Due to the lack of space-time data density of the existing data, the effect of traditional prediction methods is poor. Artificial intelligence has the ability to infer incomplete and uncertain information and can achieve high-precision wind speed prediction. In addition, artificial intelligence can also summarize the knowledge and experience of experts, improve the average prediction level, and use the abstract prediction knowledge that cannot be used in statistical and numerical models to comprehensively consider multiple influencing factors, so as to improve the prediction level and operation efficiency of the model.

In recent years, in the research field of wind speed prediction at home and abroad, the application of artificial intelligence has increased significantly, and it shows a trend from traditional machine learning to deep learning. Wind speed is fluctuant and random, which makes wind

Fig. 7 (**a–b**) VMD decomposition results of different wind farms. (**a**) VMD decomposition data of Changma wind farm. (**b**) VMD decomposition data of Sotavento wind farm
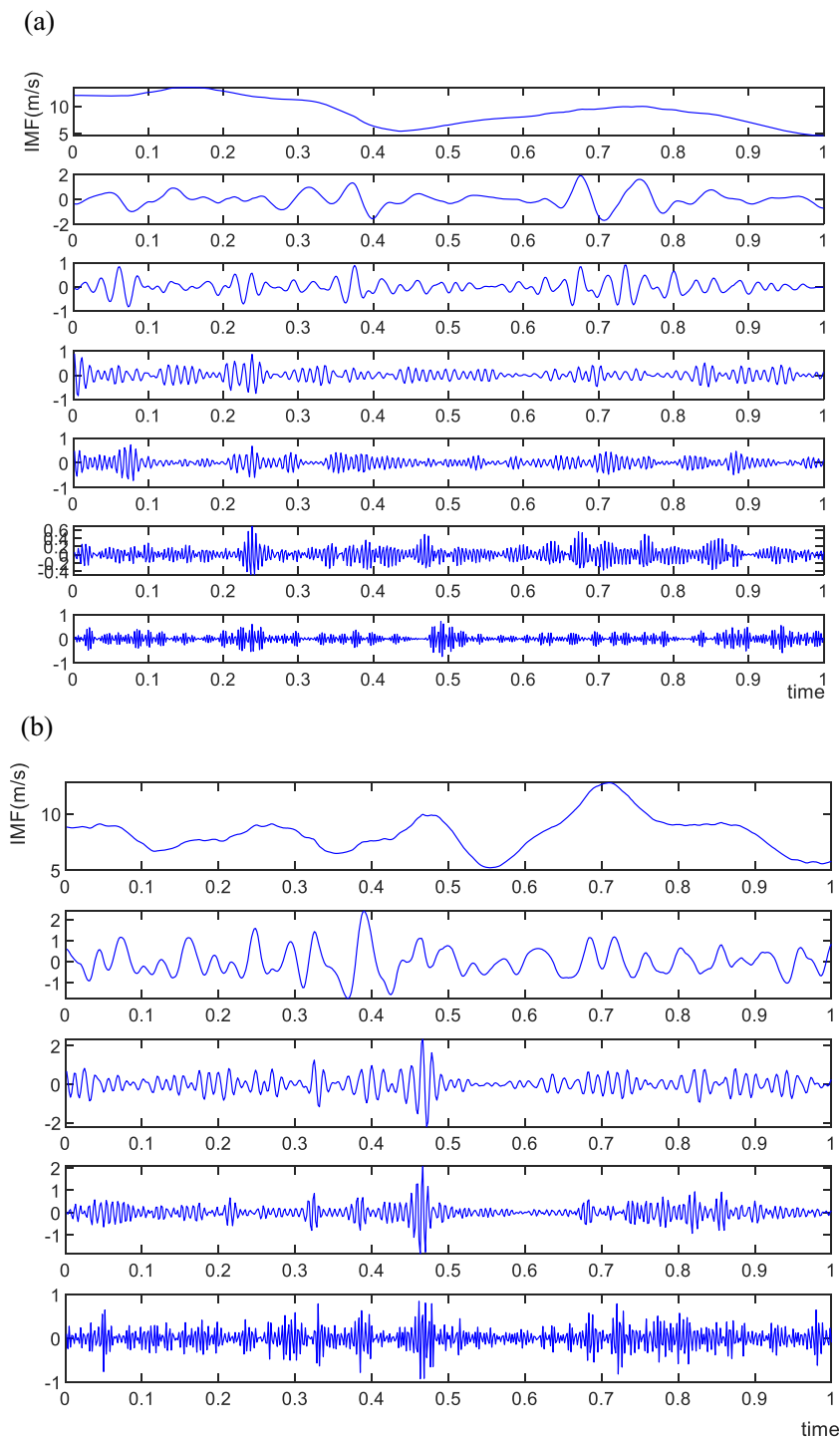
speed and wind power series highly nonlinear. Compared with traditional machine learning methods, deep learning has obvious advantages in massive data processing and nonlinear space-time prediction. It has great application potential in various technical links of wind speed simulation and prediction and provides technical support for faster, more efficient, and more accurate wind speed prediction.

Conclusion and future work

In order to reduce carbon emissions and solve environmental problems such as air pollution and ecological damage, countries around the world are developing renewable energy technologies to reduce their dependence on fossil energy. With the energy revolution facing many problems, wind power has become an important source of renewable energy, and wind
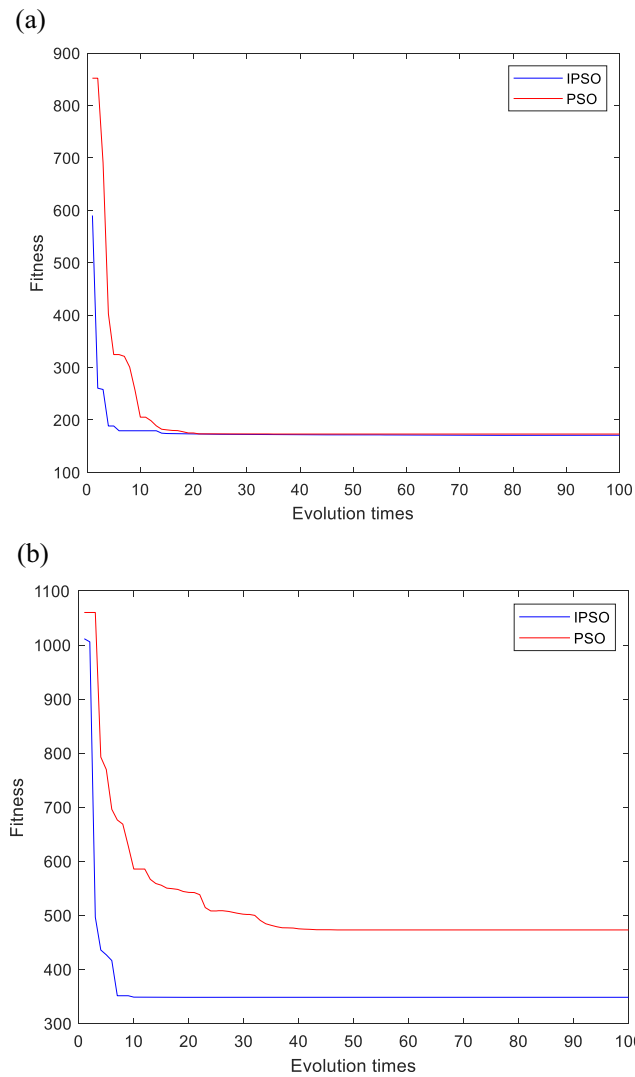
(a)

(b)

Fig. 8 Fitness curves of different wind farms. (**a**) Fitness curve of Sotavento Wind Farm. (**b**) Fitness curve of Changma Wind Farm

(a)

(b)

Fig. 9 (a–b) Wind speed prediction results of different wind farms. (**a**) Prediction results of Changma Wind Farm. (**b**) Sotavento wind Farm wind speed prediction results

forecasting technology is developing rapidly. New optimization methods and combination schemes are constantly produced. High-precision wind speed prediction method provides a scientific basis for realizing smart power grid and improving economic benefits of wind farms.

In order to achieve high-precision wind power prediction, this paper proposes an HMD-IPSO-LSTM-ARMA-E prediction scheme based on the improved VMD method and IPSO-LSTM neural network, which is verified by the wind speed data of Changma wind farm in China and Sotavento wind farm in Spain. The main experimental results are as follows:

(1) The HMD method is used to decompose the non-stationary wind speed time series, and the relatively stationary components and residual terms are obtained, which effectively solves the problems of the insignificant periodic characteristics of the wind speed time
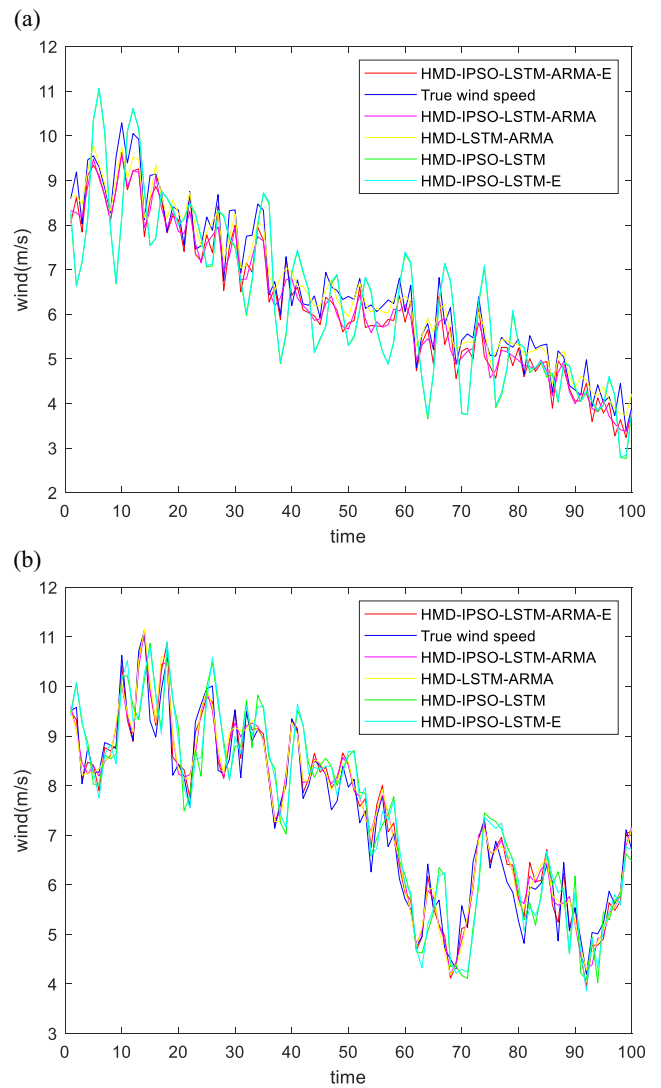
series and the difficulty in choosing the VMD mode number.

(2) Considering that as an improved RNN, LSTM neural network not only has the ability of analyzing time series

Table 5 Prediction error analysis table

Prediction model	Changma			Sotavento		
	MAE	MSE	RMSE	MAE	MSE	RMSE
H-I-L-A-E	0.2382	0.0837	0.2892	0.2165	0.0703	0.2651
H-I-L-A	0.3436	0.1565	0.3955	0.2969	0.1438	0.3793
H-L-A	0.3938	0.2284	0.4780	0.3034	0.1472	0.3836
H-I-L	0.8026	0.9828	0.9914	0.5792	0.5023	0.7087
H-I-L-E	0.7923	0.9651	0.9824	0.5308	0.4419	0.6648

Table 6 Prediction error analysis table

	MAE	MSE	RMSE
LSTM	0.2759	0.1132	0.3364
RBF	0.3560	0.1854	0.4305
Elman	0.3609	0.1926	0.4389
BP	0.4157	0.2848	0.5337

data but also has the ability of long-term memory, using IPSO to optimize the parameters of LSTM neural network which can improve the prediction accuracy of neural network.

(3) The ARMA model can take into account the dependence of time series and the disturbance caused by random fluctuation in the prediction and has a high accuracy in the short-term trend prediction. In this paper, LSTM neural network and ARMA model are specifically used to train and forecast the decomposed nonlinear wind speed sequence and linear wind speed sequence, respectively, and the prediction effect is significantly improved.

The results of the improved VMD method, the optimization of LSTM neural network, the difference analysis of different sequences, and the multiple noise decomposition are satisfactory. The combined model highlights the advantages of each algorithm, and the wind speed prediction system has more perfect wind speed processing and smaller prediction error.

In the follow-up prediction work, consider improving the quality of model input data, using NWP data with higher resolution and combining with geographic information system to correct wind speed, fully consider the impact of geographical conditions on wind speed, improve accuracy, further study wind speed series prediction based on other deep
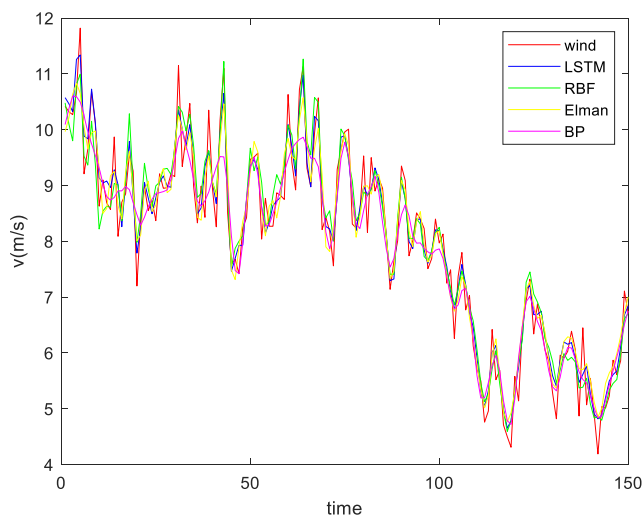
learning algorithms, try to use more optimization algorithms to improve the performance of the model, consider that the combination model combined with physical model, dynamic model, and fluid mechanics model is constructed to improve the prediction accuracy and efficiency.

Abbreviation *ANN,* Artificial neural network; *ARMA,* Autoregressive moving average; *ARIMA,* Autoregressive integrated moving average; *BP,* Back propagation; *CEEMDAN,* Fully integrated empirical mode decomposition; *EMD,* Empirical mode decomposition; *EEMD,* Set empirical mode decomposition; *FCBF,* Fast correlation filter algorithm; *HMD,* Hybrid mode decomposition; *LIDAR,* Light detection and ranging; *LSTM,* Long- and short-term memory neural network; *IMF,* Intrinsic mode functions; *IPSO,* Improved particle swarm optimization; *MAE,* Mean absolute error; *MIV,* Mean impact value; *MSE,* Mean square error; *MAPE,* Mean absolute percentage error; *NCL-RELM,* Negative correlation learning-based regularized extreme learning machine ensemble model; *NWP,* Numerical weather prediction; *OVMD,* Optimal variational mode decomposition; *PSO,* Particle swarm optimization; *RBF,* Radial basis function; *RMSE,* Root mean square error; *RNN,* Cyclic neural network; *SODAR,* Sound detection and ranging; *SVM,* Support vector machine; *VMD,* Variational mode decomposition; *WT,* Wavelet transform; *WD,* Wavelet decomposition; *WPD,* Wavelet packet decomposition

Availability of data and materials The datasets used or analyzed during the current study are available from the corresponding author on reasonable request.

Author contribution Yagang Zhang: Conceptualization, methodology, software, and writing original draft. Ruixuan Li: Methodology and performed the experiments. Jinghui Zhang: Writing review and editing

Declarations

Ethics approval and consent to participate   Not applicable

Consent for publication   Not applicable

Competing interests   The authors declare no competing interests.

Fig. 10 Comparison of the results of different prediction methods

References

Chen B (2020) Short term wind power forecasting based on wind speed characteristics analysis. North China Electric Power University

Cao YK, Hu QQ, Shi H, Zhang Y (2019) Prediction of wind power generation base on neural network in consideration of the fault time. IEEJ Trans Electr Electron Eng 14(5):670–679. https://doi.org/10.1002/tee.22853

Chaurasiya PK, Warudkar V, Ahmed S (2017) Wind characteristics observation using Doppler-SODAR for wind energy applications.

Resource-Efficient Technol 3(4):495–505. https://doi.org/10.1016/j.reffit.2017.07.001

Chaurasiya PK, Warudkar V, Ahmed S (2018a) Comparative analysis of Weibull parameters for wind data measured from met-mast and remote sensing techniques. Renew Energy 115:1153–1165. https://doi.org/10.1016/j.renene.2017.08.014

Chaurasiya PK, Warudkar V, Ahmed S (2018b) Study of different parameters estimation methods of Weibull distribution to determine wind power density using ground based Doppler SODAR instrument. Alexandria Eng J 57(4):2299–2311. https://doi.org/10.1016/j.aej.2017.08.008

Chaurasiya PK, Warudkar V, Ahmed S (2019) Wind energy development and policy in India: a review. Energy Strategy Rev 24:342–357

Chitsaz H, Amjady N, Zareipour H (2015) Wind power forecast using wavelet neural network trained by improved Clonal selection algorithm. Energy Convers Manag 89:588–598. https://doi.org/10.1016/j.enconman.2014.10.001

Dang XJ, Chen HY, Jin XM. (2013) A method for forecasting short-term wind speed based on EMD and SVM. 2645:622-627. https://doi.org/10.4028/www.scientific.net/AMM.392.622

Dragomiretskiy K, Zosso D (2014) Variational mode decomposition. IEEE Trans Signal Process 62:531–544. https://doi.org/10.1109/TSP.2013.2288675

Erdem E, Shi J (2011) ARMA based approaches for forecasting the tuple of wind speed and direction. Appl Energy 88:1405–1414. https://doi.org/10.1016/j.apenergy.2010.10.031

Glowacz A (2018) Acoustic-Based Fault Diagnosis of Commutator Motor. Electronics 299. https://doi.org/10.3390/electronics7110299

Glowacz A (2019) Fault diagnosis of single-phase induction motor based on acoustic signals. Mech Syst Signal Process 117:65–80. https://doi.org/10.1016/j.ymssp.2018.07.044

Glowacz A, Glowacz W (2018) Vibration-based fault diagnosis of commutator motor. Shock and Vibration 1–10. https://doi.org/10.1155/2018/74604192018/7460419

Gu B, Zhang TR, Meng H et al (2020) Short-term forecasting and uncertainty analysis of wind power based on long short-term memory, cloud model and non-parametric kernel density estimation. Renew Energy 164:687–708. https://doi.org/10.1016/j.renene.2020.09.087

Harty TM, Holmgren WF, Lorenzo AT, Morzfeld M (2019) Intra-hour cloud index forecasting with data assimilation. Sol Energy 185:270–282. https://doi.org/10.1016/j.solener.2019.03.065

Higashiyama K, Fujimoto Y, Hayashi Y (2018) Feature extraction of NWP data for wind power forecasting using 3D-convolutional neural networks. Energy Procedia 155:350–358. https://doi.org/10.1016/j.egypro.2018.11.043

Hodge B-M, Zeiler A, Brooks D, Blau G, Reklatis G (2011) Improved wind power forecasting with ARIMA models. Comp Aided Chem Eng 29:1789–1793. https://doi.org/10.1016/B978-0-444-54298-4.50136-7

Hu H, Lin W, Lv S-X (2020) Forecasting energy consumption and wind power generation using deep echo state network. Renew Energy 154:598–613. https://doi.org/10.1016/j.renene.2020.03.042

International Renewable Energy Agency's (IRENA). (2020) 2020 Annual renewable energy report [EB/OL], https://www.iea.org/, 2020-4-13 /2020-10-20.

Li YF, Shi HP, Han FZ, Liu H (2019a). Smart wind speed forecasting approach using various boosting algorithms, big multi-step forecasting strategy. 135540-553. https://doi.org/10.1016/j.encon.man.2017.05.063

Li YN, Yang P, Wang HJ (2019b) Short-term wind speed forecasting based on improved ant colony algorithm for LSSVM. Clust Comput 22:11575–11581. https://doi.org/10.1007/s10586-017-1422-2

Liu H, Duan Z, Han FZ, Li YF (2018a) Big multi-step wind speed forecasting model based on secondary decomposition, ensemble method and error correction algorithm. Energy Convers Manag 156:525–541. https://doi.org/10.1016/j.enconman.2017.11.049

Liu H, Mi XW, Li YF (2018b) Comparison of two new intelligent wind speed forecasting approaches based on wavelet packet decomposition, complete ensemble empirical mode decomposition with adaptive noise and artificial neural networks. Energy Convers Manag 155:188–200. https://doi.org/10.1016/j.enconman.2017.10.085

National Energy Administration. (2020) Transcript of national energy administration's online press conference in the third quarter of 2020 [EB/OL], http://www.nea.gov.cn/

Nazir MS, Ali ZM, Bilal M, Sohail HM, Iqbal HMN (2020a) Environmental impacts and risk factors of renewable energy paradigm—a review. Environ Sci Pollut Res 27:1–11. https://doi.org/10.1007/s11356-020-09751-8

Nazir MS, Bilal M, Sohail HM, Liu B, Wan C, Iqbal HMN (2020b) Impacts of renewable energy atlas: reaping the benefits of renewables and biodiversity threats. Int J Hydrog Energy 45:22113–22124. https://doi.org/10.1016/j.ijhydene.2020.05.195

Nourani Esfetang N, Kazemzadeh R (2018) A novel hybrid technique for prediction of electric power generation in wind farms based on WIPSO, neural network and wavelet transform. Energy 149:662–674. https://doi.org/10.1016/j.energy.2018.02.076

Peng T, Zhang C, Zhou J, Nazir MS (2020) Negative correlation learning-based RELM ensemble model integrated with OVMD for multi-step ahead wind speed forecasting. Renew Energy 156:804–819. https://doi.org/10.1016/j.renene.2020.03.168

Shahid F, Zameer A, Mehmood A, et al. (2020) A novel wavenets long short-term memory paradigm for wind power prediction. 269. https://doi.org/10.1016/j.apenergy.2020.115098

Sharifian A, Ghadi MJ, Ghavidel S, Li L, Zhang JF (2018) A new method based on type-2 fuzzy neural network for accurate wind power forecasting under uncertain data. Renew Energy 120:220–230. https://doi.org/10.1016/j.renene.2017.12.023

Skittides C, Früh W-G (2014) Wind forecasting using principal component analysis. Renew Energy 69:365–374. https://doi.org/10.1016/j.renene.2014.03.068

Tang B, Chen Y, Chen Q et al (2020) Research on short-term wind power forecasting by data mining on historical wind resource. Appl Sci 10(4):1295. https://doi.org/10.3390/app10041295

Tian Z, Ren Y, Wang G (2019) Short-term wind speed prediction based on improved PSO algorithm optimized EM-ELM. Energy Sources Part A: Recovery, Utilization, and Environmental Effect 41(1):26–46

Wang SX, Zhang N, Wu L et al (2016) Wind speed forecasting based on the hybrid ensemble empirical mode decomposition and GA-BP neural network method. Renew Energy 94:629–636. https://doi.org/10.1016/j.renene.2016.03.103

Wang SX, Li M, Zhao L et al (2019) Short-term wind power prediction based on improved small-world neural network. Neural Comput & Applic 31:3173–3185. https://doi.org/10.1007/s00521-017-3262-7

Wu JS, Long J, Liu MZ (2015) Evolving RBF neural networks for rainfall prediction using hybrid particle swarm optimization and genetic algorithm. Neurocomputing 148:136–142. https://doi.org/10.1016/j.neucom.2012.10.043

Yu CJ, Li YL, Zhang MJ (2017) An improved wavelet transform using singular spectrum analysis for wind speed forecasting based on Elman neural network. Energy Convers Manag 148:895–904

Yuan XH, Chen C, Yuan YB, Huang YH, Tan QX (2015) Short-term wind power prediction based on LSSVM–GSA model. Energy Convers Manag 101:393–401. https://doi.org/10.1016/j.enconman.2015.05.065

Zafirakis D, Tzanes G, Kaldellis JK (2019) Forecasting of wind power generation with the use of artificial neural networks and support vector regression models. Energy Procedia 159:509–514. https://doi.org/10.1016/j.egypro.2018.12.007

Zendehboudi A, Baseer MA, Saidur R (2018) Application of support vector machine models for forecasting solar and wind energy resources: a review. J Clean Prod 199:272–285. https://doi.org/10.1016/j.jclepro.2018.07.164

Zhang YG, Pan GF (2020) A hybrid prediction model for forecasting wind energy resources. Environ Sci Pollut Res 16:19428–19446

Zhang DL, Li SS, He XD (2015) RBF neural network wind power prediction based on chaos theory. Adv Mater Res 3701:315–318. https://doi.org/10.4028/www.scientific.net/AMR.1070-1072.315

Zhang L, Wang K, Lin WL, et al. (2019a) Wind power prediction based on improved genetic algorithm and support vector machine. 252(3)

Zhang YG, Chen B, Pan GF, Zhao Y (2019b) A novel hybrid model based on VMD-WT and PCA-BP-RBF neural network for short-term wind speed forecasting. Energy Convers Manag 195:180–197. https://doi.org/10.1016/j.enconman.2019.05.005

Zhang Y, Zhang C, Gao S, Wang P, Xie F, Cheng P, Lei S (2020a) Wind speed prediction using wavelet decomposition based on lorenz disturbance model. IETE J Res 66:635–642. https://doi.org/10.1080/03772063.2018.1512384

Zhang YG, Pan GF, Chen B, Han JY, Zhao Y, Zhang CH (2020b) Short-term wind speed prediction model based on GA-ANN improved by VMD. Renew Energy 156:1373–1388

Zhang YG, Pan GF, Zhao YP, Qian L, Wang F (2020c) Short-term wind speed interval prediction based on artificial intelligence methods and error probability distribution. Energy Convers Manag 224:1–14

Zhang Y, Han J, Pan G, Xu Y, Wang F (2021) A multi-stage predicting methodology based on data decomposition and error correction for ultra-short-term wind energy prediction. J Clean Prod 292:1–19. https://doi.org/10.1016/j.jclepro.2021.125981

Zhao QD, Yu Y, Jia MM. (2014) Applied-information technology in short-term wind speed forecast model for wind farms based on ant colony optimization and bp neural network. 3563:259-262. https://doi.org/10.4028/www.scientific.net/AMM.662.259

Publisher's note Springer Nature remains neutral with regard to jurisdictional claims in published maps and institutional affiliations.